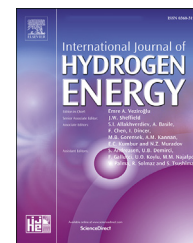


Available online at www.sciencedirect.com

ScienceDirect

journal homepage: www.elsevier.com/locate/hydro

High-pressure gaseous hydrogen permeation test method -property of polymeric materials for high-pressure hydrogen devices (1)-

Hirotda Fujiwara ^{a,*}, Hiroaki Ono ^a, Kiyoaki Onoue ^a, Shin Nishimura ^{a,b}

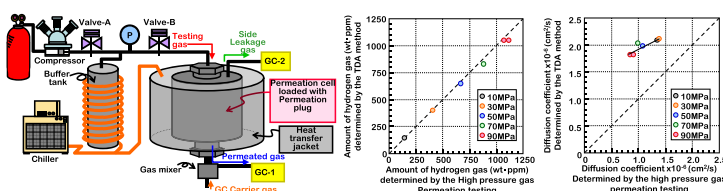
^a Research Center for Hydrogen Industrial Use and Storage Kyushu University (HYDROGENIUS), HY-10, 744 Motoooka, Nishi-ku, Fukuoka 819-0395, Japan

^b Department of Mechanical Engineering in Faculty of Engineering, Kyushu University, Japan

HIGHLIGHTS

- High pressure hydrogen gas permeation test device was developed.
- Evaluation of polymer permeation in equilibrium state up to 100 MPa is possible.
- Advantage of the method was compared with the non-equilibrium state method.
- Hydrogen permeability deteriorates with the increase of gas pressure.
- Hydrostatic compression effect can affect diffusion deterioration under higher pressure.

GRAPHICAL ABSTRACT



ARTICLE INFO

Article history:

Received 13 June 2020

Received in revised form

19 July 2020

Accepted 23 July 2020

Available online 21 August 2020

Keywords:

High-pressure gas seal

Gas permeation

ABSTRACT

Polymeric materials are widely used in hydrogen energy system such as FCEV and hydrogen refueling stations under high-pressure condition. The permeation property (coefficients of permeation, diffusion and solubility) of polymers under high-pressure hydrogen condition should be discussed as parameters to develop those devices. Also the property should be determined to understand influence of the compression by the pressure on polymer materials. A device which can measure gas permeation property of polymer materials accurately in equilibrium state under high-pressure environment is developed, and the reliability of the measurements is ensured. High-pressure hydrogen gas permeability characteristics up to 100 MPa are measured for high-density polyethylene. An advantage of the method is discussed comparing with the non-equilibrium state method,

* Corresponding author.

E-mail addresses: fujiwara.hirotda.835@m.kyushu-u.ac.jp (H. Fujiwara), ono.hiroaki.340@m.kyushu-u.ac.jp (H. Ono), onoue.kiyoaki.852@m.kyushu-u.ac.jp (K. Onoue), nishimura.shin.691@m.kyushu-u.ac.jp (S. Nishimura).

<https://doi.org/10.1016/j.ijhydene.2020.07.215>

0360-3199/© 2020 The Author(s). Published by Elsevier Ltd on behalf of Hydrogen Energy Publications LLC. This is an open access article under the CC BY-NC-ND license (<http://creativecommons.org/licenses/by-nc-nd/4.0/>).

Gas diffusion
Gas solubility
Storage tanks
Dispensing hoses

focusing on the hydrostatic pressure effect. Deterioration of hydrogen permeability is observed along with the decrease of diffusion coefficient, which is supposedly affected by hydrostatic compression effect with the increase of environment pressure.

© 2020 The Author(s). Published by Elsevier Ltd on behalf of Hydrogen Energy Publications LLC. This is an open access article under the CC BY-NC-ND license (<http://creativecommons.org/licenses/by-nc-nd/4.0/>).

Introduction

Recently, hydrogen energy system has been paid much attention as a solution to fossil fuel depletion and environmental issues [1], since hydrogen does not deteriorate regardless of long term storage, and is able to generate a large power, it has been put into practical use as an energy carrier medium [2]. Nevertheless, fossil fuel such as gasoline is still dominant energy especially for transportation sector. In order to convert the fuel of the vehicles, electric vehicles, such as battery electric vehicles (BEV) and fuel cell electric vehicles (FCEV) are much attracted for the decades. Since 2014, FCEVs have been on the market and have been gradually disseminated in US, EU countries, Korea and Japan. In these countries, hydrogen refueling stations (HRS) are developed. Because of low energy density of gaseous hydrogen, the hydrogen is compressed up to 70 MPa and stored in the high-pressure hydrogen vessels on the vehicle. In order to promote the dissemination of the FCEV, mass-production and cost-reduction of the high-pressure hydrogen devices and storage tanks are required [3]. In these devices and storage tanks, polymeric materials are used for the sealing devices such as O-rings or gaskets, inner liners for the type 4 tanks on the vehicle and the flexible hydrogen dispensing hoses of HRS. These polymeric materials are directly exposed to the high-pressure hydrogen and are should to seal or barrier the high-pressure hydrogen. For example, international standard for the type 4 tank in GTR 13 requires the hydrogen permeation to be less than $46 \text{ Ncm}^3 \text{ h}^{-1} \text{ dm}^{-3}$ at 70 MPa, 55 °C [4]. ISO19880-5 requires that the permeation amount of hydrogen form the flexible dispensing hose to be less than $500 \text{ Ncm}^3 \text{ h}^{-1} \text{ m}^{-1}$ at 87.5 MPa. HySafe proposed a basic method to estimate an allowable upper limit for hydrogen permeation in automotive applications, and a maximum hydrogen permeation ratio from road vehicles into enclosed structures [5]. To design the type 4 tank or hydrogen hoses, suitable materials shall be selected, based on the hydrogen permeability of the inner liner polymeric materials simulating the condition under high-pressure environment of practical use. Hydrogen permeability, diffusivity, and penetrability are important parameters for designing or selecting the materials suitable for those usage [6]. For the purpose, development of direct measurement method of hydrogen permeability is necessary. Although there is a report about hydrogen permeation coefficients of epoxy resin with glass lacquer, aiming to enable long-term storage of hydrogen in tanks, the pressure applied in the test was as low as 1.5 bar (0.15 MPa) [7]. But the evaluation of permeability under the pressure in the type 4 on-board tank or for the practical operation pressure of

HRS is limited to the study using practical parts such as tanks or hoses [8].

In this study, hydrogen permeability measurement system for high-pressure hydrogen up to 90 MPa has been developed.

Our research group are continuously working on the analysis of the polymeric materials for the sealing or barrier materials for high-pressure hydrogen devices. In our previous study, it has been already reported that hydrogen absorbed in rubber by high-pressure hydrogen exposure initiates bubbles during decompression, resulting in fracture such as blister, overflow and buckling due to the inflation of the rubber materials [9–12]. Furthermore, the inflated polymeric materials by the high-pressure hydrogen exposure shrink after the hydrogen elimination by decompression. The polymeric materials are inflated and contracted repeatedly by the change of the pressure. Since the elastic modulus at the volume inflation state is reduced and the reduction ratio corresponds to the change in the cross-sectional area, it is concluded that the reduction in the number of molecular chains responsible for the elastic modulus per unit area due to volume expansion is not the result of hydrogen affecting the rubber molecular motion [13]. It is also reported that, despite the chemical structure is not changed by the repeated exposure and decompression, the physical deterioration such as the decrease of filler network and the boundary rubber layer progresses, resulting the lowering of the elastic modulus [14]. We also reported a quantitative evaluation method using an attenuation of the amount of light as an index of the state of the blister fracture [15].

Polymeric materials such as crystalline polymers or rubber materials have free volume between molecular chains caused by the segmental motion of the molecules. Therefore, the hydrogen gas easily penetrates into and permeates from the material. Numbers of studies have been conducted on the gas permeability of polymeric materials. Salame reported “Permachor parameter” calculated from empirically derived factors for each chemical group in the polymer repeat unit to derive gas-permeability coefficients based on free volume fractions and aggregation density energies [16]. A calculation method considering the cohesive energy, packing, and rotational degrees of freedom of the polymer is derived by Bicerano et al. [17]. Besides them, Paul et al. calculated the free volume fraction based on the occupied volume and density calculations and reported that the result can be used for predicting the gas permeability as the earned free volume fraction showed good correlations with the gas permeability [18].

As typical early studies on gas permeation in pressurized environments there are reports by Henly et al., Stern et al. and Li et al. on PEs and PPs [19–25]. Henry evaluated the

permeability of inorganic and organic gases at pressurization conditions of up to about 200 psi (1.4 MPa), and Li up to 1500 psi (10 MPa). They proved that the permeation coefficients in logarithmic notation show linearity with pressurization pressure and that the relation of pressure to permeability differs depending on the gas species. Li evaluated the dissolution amount and reported that the linear approximation of the low pressure was manifested and the Henry's law was applicable below the critical pressure, but the considerable deviation occurred above the critical pressure. Stern have analyzed the permeation behavior of inorganic gas e.g. hydro olefins and Fluor olefin-based organic gases up to 54.4 atm (5.5 MPa) under the conditions of 18 °C–70 °C and discussed the relation to free volume. It is explained that the cause of change in permeation coefficient with pressurization is the effect of correlation between the increased free volume due to the absorption of penetrant and the decrease of free volume due to hydrostatic compression. Naito et al. proposed a method to divide the pressure dependency of permeability into two factors related to hydrostatic pressure and concentrations by considering the effects of gas molecular sizes and solubility on diffusions [26,27].

When high-pressure gas is applied to one side of polymer materials, there is a possibility of the increases in permeation driving force, reduction in free volume, and progress of plasticization. Those phenomena can affect permeation property of the materials interacting each other in a complicated manner. It will be easily understood that actual measurement of the permeation behavior under practical hydrogen pressure above 80 MPa is indispensable.

Currently, there are equipments to measure the gas permeability characteristic in a high-pressure gas equilibrium state up to 130 atm (about 13 MPa), but there is no reports of actual evaluation for polymer materials in such a high-pressure environment [26]. This is because there is no apparatus which can analyze materials in a high-pressure equilibrium state. There are several potentially applicable measurement methods. For example, an equipment consists of high-pressure compartment, and the compartment in which a sample is held, divided by a valve to evaluate gas absorption and a diffusion coefficient. In this method, internal pressure is measured which decreases according with the gas amount absorbed into the specimen, comparing with the space volume measured after the gas is released [28,29]. However, this method needs a pressure gauge which can measure very wide and dynamic range of pressure accurately for the evaluation at high-pressure condition. For example, to detect some hPa conversion under high-pressure condition as high as 100 MPa. The absence of those accurate pressure gauge makes it difficult to apply the method for the evaluation at high-pressure condition.

The volume of the sample changes under hydrostatic high-pressure, and true value of diffusion coefficient of the sample cannot be calculated. Absorption behavior measurement method using a magnetic suspension balance is also considered as a candidate [30]. In this case, it is necessary to provide a measuring instrument with such high precision that a change of several tens of ppm in weight ratio can be observed. It is necessary to measure only the true specimen weight change without drift even when a material is highly

pressurized instantaneously to determine the diffusion coefficient. Another method is measuring by using electrical properties such as piezoelectric electro sorption in the limit of 10 MPa [31]. The reasons why this method can not be applied for high-pressure hydrogen gas is that sealing property can not be secured where the electric wiring is installed and that the wiring can be deteriorated by the hydrogen gas. In short, there are currently no measuring instruments that satisfy those necessary requirements.

We have also proposed a thermal desorption analysis (TDA) method for measuring the amount of gas penetration and the diffusion coefficient in a non-equilibrium state by measuring hydrogen eliminated from a polymeric material after decompression following high-pressure hydrogen exposure by gas chromatograph [11,32,33]. The TDA method is a convenient method for determination of amount of penetrated gas and the diffusion coefficient of the sample. However, the method is controversial about the influence of the environment in which the test specimen is placed after decompression, and it has not been judged whether or not the extrapolated value is a true value.

We have developed a system capable of permeation test in equilibrium state for polymeric materials with high-pressure gases up to 100 MPa, especially hydrogen gas which is easy to leak. Advantage of this system is that sheet-shaped specimens can be used, that is, easy to prepare with various materials, and easy to determine thickness, i.e. permeation distance, and permeation area. Determination of thickness and area is essential to earn coefficients such as permeability, diffusion, and solubility for relative assessment of the polymer materials. The structure of the equipment enables to contribute to get accurate and reliable data, preventing deformation of the samples. In this paper, the gas permeation behavior at high-pressure in equilibrium state and determination of the permeability and amount of absorbed hydrogen are described. As a model material, high-density polyethylene was selected, which is not affected by humidity and molding conditions, and has been reported a lot, not practical materials which is difficult to be supplied and disclosed. The results are compared with those by TDA method. The evaluation of the reliability of the equipment is also described.

Experimental

Basic theory of permeation tests

To evaluate the gas permeation property, a differential pressure method has been reported by Barrer, Kammermeyer, Amerongen [34–36]. The method has been standardized in ASTM1434 and ISO7229, and many evaluations applied the method have been reported [8]. In the method, permeation coefficient, diffusion coefficient, and solubility coefficient showing the amount of absorbed gas were analyzed based on the permeation behavior of the gas penetrates through the specimen set between a high-pressure cell and a low-pressure cell. The gas permeation amount per unit time is measured until the permeated gas reaches steady state, and value normalized by permeation area, test pressure, and test temperature is expressed as a gas permeability GP [mol/

($\text{m}^2 \cdot \text{s} \cdot \text{Pa}$)). By normalizing gas permeability with the permeation distance, the value converted into the gas permeation coefficient, and is expressed by the following equation.

$$P = GP \times d \quad (1)$$

where P is the permeation coefficient [$\text{mol} \cdot \text{m} / (\text{m}^2 \cdot \text{s} \cdot \text{Pa})$], and d is the specimen thickness [m],

$$GP = \frac{273.15 \times V}{A \times \Delta p \times T \times 0.0227} \quad (2)$$

where V is the Amount (volume) of gas permeated to the low-pressure side in the steady state [cm^3/sec], A is the permeation area [m^2], Δp is the pressure difference (Pa), and T is temperature (K).

In this method, the permeation coefficient can be obtained by quantifying the permeated gas. Since the permeation coefficient is derived from the actual amount of permeated gas, it is more reliable than with the volume method described above.

When the time dependency of the permeated gas amount is drawn as an integral curve (the horizontal axis is time, the vertical axis is total amount of the permeated gas), and the intersection point when the straight line section indicating the steady state is extrapolated to the time axis is “time-lag” θ , the diffusion coefficient can be expressed by the following equation.

$$D = \frac{l^2}{6\theta} \quad (3)$$

where D denotes the diffusion coefficient (cm^2/s).

Further, the solubility coefficient in which the amount of gas absorbed per unit volume of the test specimen normalized by pressure is expressed by the following equation.

$$S = \frac{P}{D} \quad (4)$$

where S is the solubility coefficient ($\text{mol}/\text{m}^3 \cdot \text{Pa}$).

Although there have been reports about high-pressure permeation tests using practical tanks [8] or metal plates [37] to evaluate gas permeation property, there have been no reports for permeation tests using polymer sheet materials. The thickness and permeation area of the specimens should be specified to calculate each coefficient.

Important conditions for the test under a high-pressure environment include: 1: stability of the permeation area of the test specimen in high-pressure environment; 2: accurate determination of the thickness of the sample, which is the permeation distance l ; 3: instantaneous pressurization of the specimen to the target pressure to determine the accurate time-lag; 4: avoidance of gas leakage in the condition of instantaneous pressurization and the damage of test specimen; and 5: the stability of the temperature in the whole system.

System overview of the high-pressure permeation test equipment

As shown in Fig. 1(a), the high-pressure permeation tester consists of a 100 MPa-class compressor, buffer tank (500 cc), pressure gage, and a permeation cell that holds the test

specimen when high-pressure gas is applied (permeation plugs are inserted therein), an auto gas sampler that collects the carrier gas with permeated gas at regular intervals and introduces it into gas chromatography, and a gas chromatography system that can measure the amount of permeated gas in the carrier gas. The chiller circulates the heat medium to adjust the temperature of the gas to a test temperature in advance, and the gas is maintained at the test temperature during the measurement. The high-pressure gas shut-off valves A and B which can be opened and closed instantaneously are provided on the gas piping. A safety valve is equipped between the gas mixture and gas chromatography to provide against unexpected excessive pressure over 1 MPa. Pressure gauge: KJ16-6FH [Nagano-keiki CO. LTD.] with NR-TH08 and KFD2-STC4-Ex1 (accuracy $\pm 0.5\%$). Thermometer: EXS-T [OKAZAKI MANUFACTURING COMPANY] with NR-TH08 (accuracy $\pm 0.4\%$).

High-pressure permeation cell

The high-pressure permeation cell is equipped with the Permeation plug consists of Upper bolt, Lower bolt and Frame shown in Fig. 1(b), and is designed to withstand deformation when high-pressure gases are applied from the top of the drawing with the test specimen interposed there between Sintered metal filters (porous stainless steel disc [SMC Corporation] [38]). In order to suppress deformation at the time of gas application, ring shaped anchors 0.5 mm in height are provided on the low-pressure side, and a gas-sealing O-Ring is provided on the high-pressure side. The gas permeated to the low-pressure side, shown in the lower part of the figure needs to be mixed instantaneously with the gas chromatography carrier gas with high efficiency. Correspondingly, the permeated gas is introduced as a mixed gas into the auto sampler through the outer piping while being mixed by the carrier gas (50 cc/min) flowing from below through the inside of the double tube structure in the sintered metal filter.

Specifications of the components of the system

High-pressure gas shut-off valves: [NOVA] NV1-60-6H-ATO and [Fujikin Co.Ltd.] M3R4.

Gas Chromatography: [JP-SCIENCE LAB Co.,Ltd] GC-7000-T, Column: Molecular Sieves, Analytical Period: 0.5 vol-ppm (flow-rate 50 cc/min, 4 kpa) 4 min, Detector: Thermal Conductivity Detector (TCD) Measurements, Auto sampler: [JP-SCIENCE LAB Co.,Ltd] 5 min intervals into a gas chromatograph with a GSL-700A 1 mL measuring tube.

Test procedure

The temperatures in the buffer tank and permeation cell showed in Fig. 1(a) were maintained at $30^\circ\text{C} \pm 0.2^\circ\text{C}$. Test gas from the gas supply is pressurized with a compressor to create a test pressure gas in the buffer tank with the Valve-A open and-B closed, the gas for the test cylinder pressure gas. It is necessary to pressurize with an additional pressure predicted to loose, which can be calculated from the volume of the opposite side of Valve-B. When the temperature of the gas in the buffer tank reaches the test temperature, the Valve-A is

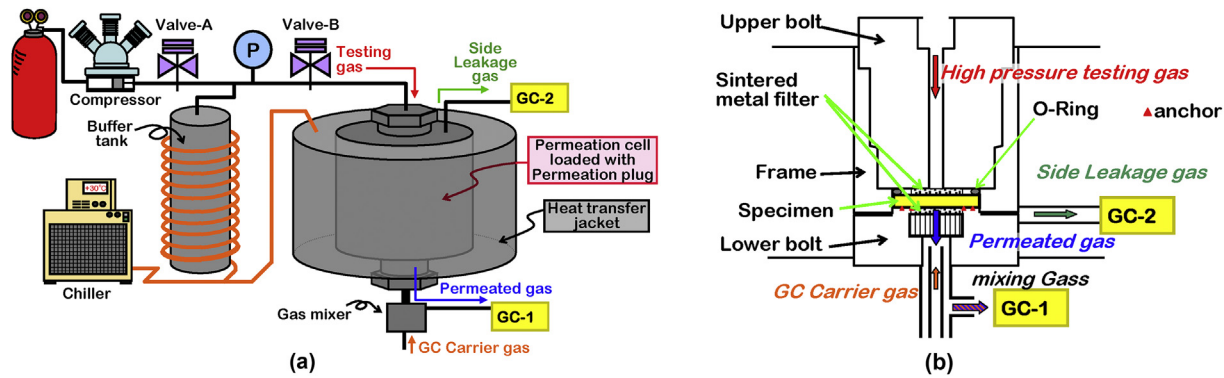


Fig. 1 – (a) Schematic of Permeation system. (b) Schematic of Permeation plug.

closed and Valve-B is opened, and the gas is instantaneously applied to the specimen. Conversion of pressure and temperature when Valve B opened is shown in [appendix Figure A1](#).

The applied gas permeates through the specimen, and the permeated gas is introduced into the gas chromatograph 1 at intervals of 5 min to be quantified. The gas permeation in the transverse direction is likewise introduced into the gas chromatograph 2 and quantified. All seal materials (O-Rings and buck-up rings) are replaced for each experiment for avoiding influence of cyclical use.

Sample

The employed material was high density polyethylene (HDPE) Novatec HB111R [Japan Polychem Corporation]. The plate specimen with the dimension of 150 mm × 150 mm × 4 mm was prepared by the hot press method according to the JIS K6922-2, Molding Temperature: 180 °C, Average Cooling Rate: 15 °C/min, Molding Pressure: 5 MPa, Pressurization Time: 5min. After preparation of the specimen, the skin layer of the plate specimen were removed by MC-working to form 1.1 mm, 1.5 mm, 2 mm, and 3.1 mm plates with surface roughness, Φ27 mm disks were punched from the plate for the experiments.

The properties of the test specimens were shown [Table 1](#).

Thermal Desorption Analyzer (TDA)

The measurement method previously reported is described here again to confirm. A disk-shaped test piece of Φ13 mm × 2 mm thickness exposed to high-pressure hydrogen is held in an electric oven held at 30 °C by a Thermal Desorption Analyzer JSH-201 [JP-SCIENCE LAB Co.,Ltd] Argon gas of 50 cc per min 4 kPa as a GC carrier gas is circulated in the electric furnace, and hydrogen gas eliminated from the specimen is sampled at intervals of 5 min and introduced into the GC to measure the concentration of the hydrogen gas. The absorbed gas in the specimen is completely eliminated by heating to 175 °C. during the elapse of 24 h. The time conversion of the remaining hydrogen amount in the specimen with the time passage is obtained from the integral curve of the elimination amount. The penetrated hydrogen amount and diffusion coefficient are obtained by fitting the

initial hydrogen amount and diffusion coefficient of zero time as unknowns from the diffusion equation shown in the formula Eq. (5).

$$C_H(t) = \frac{32}{\pi^2} \times C_{H(0)} \times \left[\sum_{n=0}^{\infty} \frac{\exp\left[(-2n+1)^2 \pi^2 D t / \ell^2\right]}{(2n+1)^2} \right] \left[\sum_{n=1}^{\infty} \frac{\exp(D \beta_n^2 t / \rho^2)}{\beta_n^2} \right] \quad (5)$$

where $C_H(t)$ is the remaining hydrogen content (wt·ppm), D is diffusion coefficient (mm²/s), β_n is the root of the zero-order Bessel function, ℓ is the thickness of sample and ρ is the radius of disk specimen.

Results

Reliability evaluation of test equipment

Examination of seal structure

In order to prove the sealing performance of the high-pressure permeation plug shown in [Fig. 1\(b\)](#), the effect of the presence or absence of anchors was examined using a 1.5 mm thick sheet specimens. In the absence of the anchor, excessive amount of lateral gas leakage was detected with test gas pressurization. On the other hand, in the seal mechanism using the anchors in combination, even when the high-pressure gas is instantaneously applied, gas leakage in the

Table 1 – The properties of the test specimens.

Density	0.942 g/cm ³
Molecular weight	Mn: 1.3 × 10 ⁴ g/mol, Mw: 2.7 × 10 ⁵ g/mol
Degree of crystallinity ^a	77–78%,
Glass transition temperature ^b	–115 °C
Tensile yield stresses	24.1 MPa
Elongation at break	818%
Modulus	645 MPa.
Surface roughness,	Ra: 1.45–2.86 μm, Rz: 10.45–17.50 μm

^a Determined by wide-angle X-ray measurement.

^b Determined by differential scanning calorimetry.

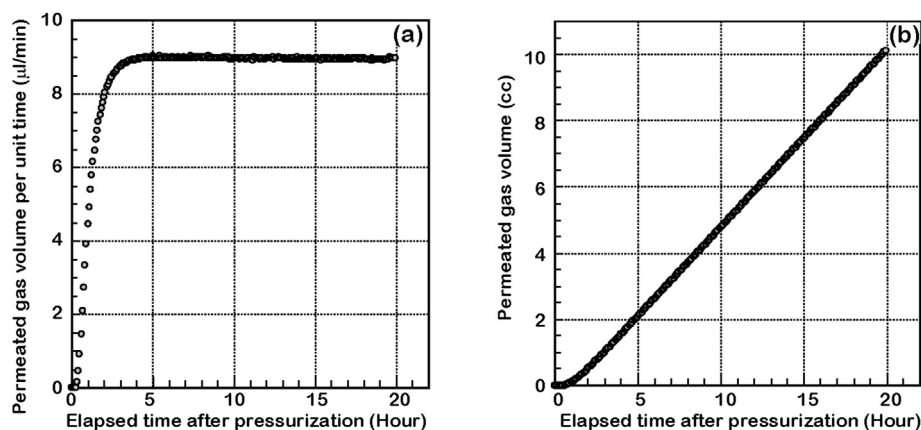


Fig. 2 – Permeation curve on 90 MPa at 30 °C Transmission side area 201 mm². (a) Differential Permeation curve (b) Integral Permeation curve.

lateral direction, which is caused by the breakage of sealing mechanism was not observed, and even when it is held for a long time, gas leakage was not detected. Transmission curve was successfully obtained as shown in Fig. 2. After about 5 h, permeation reached the steady state, after which no variation in the permeation amount is observed. 3D image of a specimen after high-pressure permeation test is shown in Fig. 3. The deformation of the specimen of polymeric material was not observed in the sealing system using the anchors, but in the mechanism using only the O-Ring, the specimen deformed. The photograph (b) depicts the deformation in the lower right part of the specimen of polymeric material along with the trace of the outward movement of the O-Ring. In the planar self-sealing system with the O-Ring, the O-Ring is pressed against the contacting surface of the specimen by a force higher than the pressure of the applied gases. As a result, the specimen of polymeric material is deformed in the outer circumferential direction and becomes thin to make a gap, then the seal mechanism cannot be secured because of the gap. Therefore, the mechanism in which the specimens deforms as in the case of the structures represented by ISO JIS-K7126it is not appropriate for the high-pressure permeation test of samples such as polymeric material or rubber. In contrast, our new system provides anchor and system to restrain the movement of the specimen and reduce the gap

with the frame, to suppress the deformation of the specimen. As a consequence, the sealing mechanism is secured, and it becomes possible to seal the hydrogen gas efficiently.

Fineness(Pore size) of the sintered metal filter

Stern et al. compared the permeability determined by using a 14 × 14 mesh steel screen and that earned by using porous stainless steel disc as a sample-holding mechanism [39]. There was a difference between the two results, and it was concluded that the permeability is greater when steel screen was used, and that the difference was greater when pressures were higher. The reasons include (1) a decrease in permeability of the porous metal support due to a decrease in effective membrane area, or (2) an increase in permeability of the screen support due to deformation of the membrane. Steel screen was not used in this test because of the large deformation of polymeric materials and the possibility of breakage, and the relation between the gas-permeability coefficient and the gas-diffusion coefficient values for the roughness of the mesh of sintered metal filters was evaluated. The results are shown in Fig. 4. Although there is a difference between the coefficient values depending on the nominal filtration accuracy, which represents the fineness of the filter, the difference is small, and a specific tendency is not found. Stern assumes that the true value is intermediate between the two values

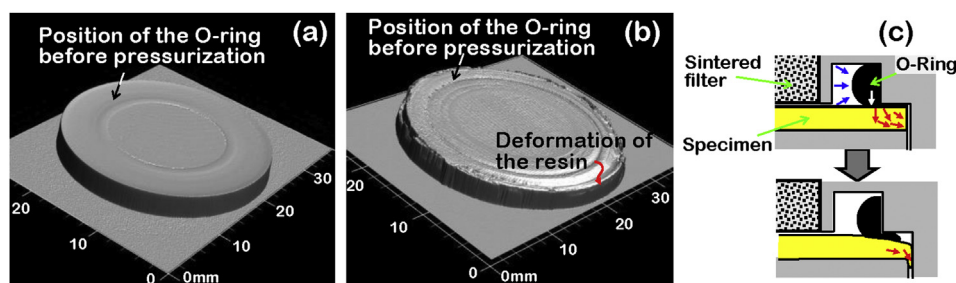


Fig. 3 – 3D image of a specimen after high-pressure permeation test. (a) Permeation plug with anchors and an O-Ring. (b) Permeation plug with only an O-Ring. (c) Schematic of O-Ring Self sealing mechanism. The O-Ring is oppressed by applied hydrogen pressure, and compresses the specimen with the pressure exceeding the applied pressure. The resin is deformed with the outward pressure by the O –Ring.

earned by the two structures, but is not necessarily true. As the influence of the use of the sintered metal filter, there were concerns about reduction of the permeation amount due to reduction of the effective area and suppression of the permeated gas diffusion, but both the permeation coefficient and the diffusion coefficient were almost unchanged in our method. It is considered that one possible cause of the stability is that even when the finest 1 μm filter is used, the permeation coefficient of the filter is several hundred times larger than the permeation coefficient of the test specimen. Moreover, the permeated hydrogen is mixed and conveyed with high efficiency by the carrier gas, and the influence of the transmission distance is negligibly small. The particle diameter used for filters with a Nominal filtration accuracy of 1 μm is 63–75 μm , the surface roughness is Ra: 7.5 μm , and the Rz: 53.7 μm is extremely larger than Rmax6.3, which ensures good sealing performance in the metallic gaskets system [40]. Since the size of the hydrogen molecules is overwhelmingly small with respect to the size of the gap formed between the particles of the filter and the specimen, it is considered that the reduction of the hydrogen permeation amount due to the presence of the filter is negligible. Even if there is an influence, the permeation value extrapolated to zero is almost equivalent to the value when 1 μm of nominal filtration accuracy was employed. Since the objective of our study is to evaluate the relatively on the basis of this method, it is judged that there is no problem to use the filter of 1 μm to perform the experiment.

Examination of permeation area

The effect of the sealing system with sintered metal filters and the combination of anchors and O-Ring was evaluated in terms of the permeation area. Various combination of the structure of the high-pressure side and the low-pressure side was examined under a pressure condition of 90 MPa using a 1.5 mm thick material as shown in Table 2. It is theoretically correct that the permeation amount increases proportionally as the permeation area increases. It suggests that no destruction or deformation of the specimen occurs in the measurement area. Fig. 5 shows the amount of permeate gas relative to the area of the permeate side (Low-pressure side), the permeation coefficient calculated based on the permeate

area, and the diffusion coefficient calculated from the time-lag. When sintered metal filters having the same permeation area are used for both the low-pressure side and the high-pressure side (black circles in the figure), the gas permeation amount shows a good proportional relationship, and the extrapolated value shows zero. When a smaller filter of $\Phi 5$ mm (permeation area 19.6 mm^2) is used, same value should be shown as the same kind of test specimen is used, but different values are shown. When a O-Ring larger than the filter in the low-pressure side was used (shown by marks in orange, green, blue), the permeation amount and permeation coefficient was as theoretical, but the diffusion coefficient showed different from the theoretical value. When the permeation area on the high-pressure side was smaller than that on the low-pressure side, the difference in the permeation amount was different, and the values of the permeation coefficient and the diffusion coefficient were also different (shown by a mark in red). This is considered to be because gas diffusion in the thickness direction is not isotropic. The above results demonstrate that gas-sealing is performed by O-Ring, and a mechanism in which the area on the low-pressure side is smaller than that on the high-pressure side must not be used. In addition, it was ensured $\Phi 5$ mm small plug having a small permeation area (19.6 mm^2) can not be used. It was also found that the structure having same area size in the low pressure side and the high-pressure side is preferable. Furthermore, it was found that the influence of the entrapment of the gas from the outer periphery in the high-pressure environment was negligible, since the extrapolated value shows zero, and it was possible to accurately determine the gas permeation area from the inner diameter of the anchor. Therefore, the system with O-Ring $\Phi 16$ mm (permeation area 201.1 mm^2), which has the largest area of this equipment, and plugs P21 was selected for further experiments.

Thickness of the specimen

Since the diffusion is proportional to the square of the thickness of the specimen, the relationship between the delay time (time-lag), which is a value for determining the diffusion coefficient, and the thickness of the specimen was evaluated. The results are shown in Fig. 6. The correlation between the

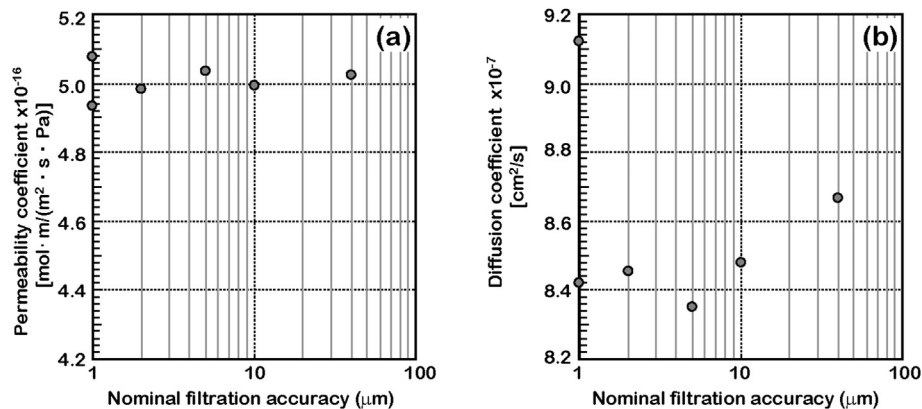
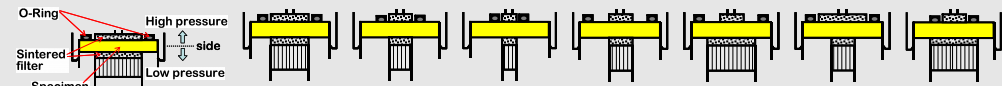


Fig. 4 – Influence of the fineness of the sintered filter. Transmission side area of high-low is 211 mm^2 , Applied pressure 90 MPa at 30 $^{\circ}\text{C}$

Table 2 – Combination of plugs with different transmission areas on the low-pressure side and high-pressure side.

Test conditions		High-Low pressure side Same transmission area				High-Low pressure side Different transmission area			
Marker		●	●	●	●	●	●	●	●
schematic of permeation plug									
High pressure side	O-Ring Inner diameter (mm)	21	18	12	9	21	21	21	12
	Sintered filter area (mm ²)	201.1	132.7	50.3	19.6	50.3	50.3	201.1	50.3
Low pressure side	Sintered filter area (mm ²)	201.1	132.7	50.3	19.6	50.3	201.1	50.3	201.1

square of the thickness of the specimen and the time-lag was confirmed, and it was judged that the specimen up to about 3 mm in thickness could be used in the present apparatus. The extrapolated value passes through zero, which is a theoretical value. This also demonstrates that the effect of the fineness of the filter does not affect the permeation mechanism. The above results indicate that the existence of the anchor does not affect the permeation distance, and it was judged our high-pressure permeation test apparatus satisfies the specifications sufficient to evaluate the gas permeability performance.

Results of the high-pressure permeation test

Fig. 7 shows the results of the high-pressure permeation test with respect to pressure (each value of the measurement is shown in appendix). The permeated hydrogen gas amount increased as the pressure increased, but the increase ratio slowed as the pressure increased. The concerned phenomena of the increase of permeation driving force was not observed. On the supposition that HDPE was used for the tank liner material, the increase ratio of the gas permeation is not as large as the increase of the pressure in the tank. The gas permeation measured with this method exhibited safer value than the one extrapolated from lower pressure value. The permeation coefficient decreased with increasing pressure,

and under the condition of 90 MPa, the permeation coefficient was approximately half of the value obtained at the time of atmospheric pressure as an extrapolated value. As reported by Li, Stern and Naito, the logarithm of permeation coefficients vs. pressures was linear, with positive slopes for highly soluble gases such as organic vapors and CO₂, and negative slopes for less soluble gases such as N₂ and He [41]. The pressure dependence of the permeability consists of a component related to the hydrostatic pressure and a component related to the concentration of the permeate gas. Li and Henley proposed plasticization of the polymer network caused by penetrant, which is the events gas penetrates into the polymers and expands the matrices, resulting in accelerated segmental motion and thereby gas diffusions [19]. The results of our approach indicate that the plasticization effects caused by hydrogen gas does not occur even at high-pressure conditions. In other words, the hydrostatic effect due to pressurization is expected to be the dominant factor of this evaluation.

The diffusion coefficient and solubility coefficient also show decreasing tendency as the pressure increases, and the ratio is slightly larger in the diffusion coefficient. It is supposed that the suppression of diffusion is a major factor of the decrease of the permeation coefficient. Penetrant is thought to move around free volume, which is a void caused by thermal vibration of the polymer chain, and to diffuse. The shrinkage of free volume under high-pressure environment is thought to

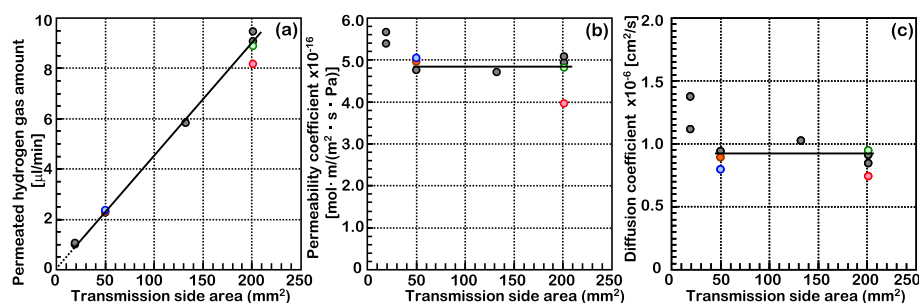


Fig. 5 – Effect of permeation area on gas permeation mechanism in 90 MPa hydrogen gas pressurization at 30 °C (a) Permeated hydrogen gas amount on stationary state. (b) Permeability coefficient (c) Diffusion coefficient.

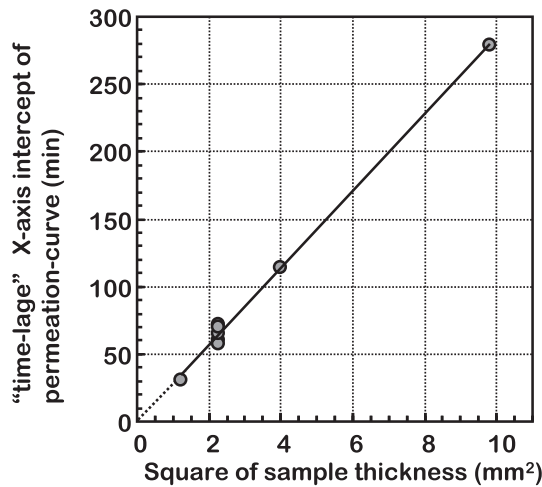


Fig. 6 – Effect of specimen thickness derived from the Relationship between specimen thickness and time-lag on gas permeation test. Transmission side area of high-low is 211 mm² and nominal filtration accuracy is 1.0 μm. Applied pressure 90 MPa at 30 °C.

be a cause of the suppression of diffusion. However, the possibility of an increase of the crystal phase, which inhibits the diffusion of the gas should be considered. The change in the fraction of free volume as an influence of the high-pressure hydrogen gas pressurization should also be considered. The change in crystallinity has been analyzed in detail by Ito et al. under hydrostatic pressure conditions [41]. Polyethylene is compressed and densified by hydrostatic pressure while maintaining the orthorhombic structure, but it is restored

quickly after decompression. It is necessary to perform measurement in an equilibrium state as it shows plasticization.

We are currently conducting high-pressure hydrogen in situ analysis of high-order structure using a high-pressure cell with a diamond window and an optical technique. Free volume fraction is evaluated based on the volume change. The details of the experiment and the results will be reported in the near future.

Comparison with TDA method

TDA method measures the desorption behavior by keeping the test specimen after the hydrogen exposure in an argon gas flow environment. Fig. 8 shows the profile of -(a) hydrogen elimination behavior, -(b) remaining hydrogen amount and -(c) remaining hydrogen amount under Argon gas environment fitted with diffusion Eq. (5), all in the HDPE specimen exposed to hydrogen at 90 MPa. The amount of hydrogen indicated by “Argon” in the figure represents the result the specimen was kept in the argon gas circulation 50 cm³ per min 4 kPa 30 °C after 10 min elapse, which is the time required for taking the specimen out of the high-pressure vessel to install in TDA. “Helium” represents the value measured by TDA after being kept under helium-flow condition (4 kPa, 50 cm³ per min.) at 30 °C for 1 h “Vacuumed” value was obtained by measuring with TDA after being kept in vacuumed condition of about 10Pa (G) with a vacuum. The amount of remaining hydrogen does not differ after 1 h regardless of the difference of the environments, and it was proven that the elimination until then was considered to be approximately equal as in vacuum.” This fact shows the hydrogen elimination behavior of HDPE is not conformity with elimination-controlling but with diffusion-controlling, and the high-pressure hydrogen

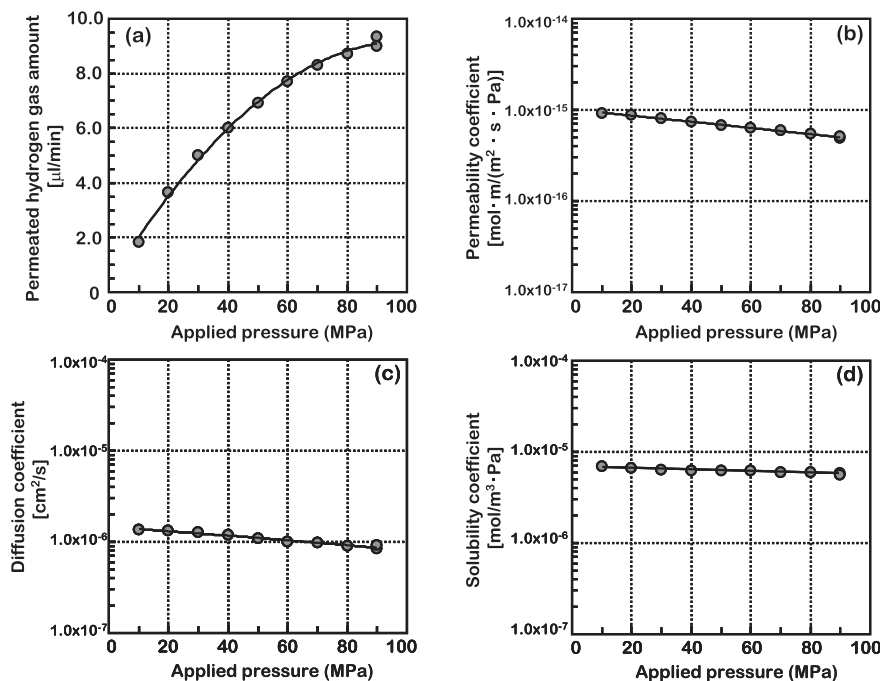


Fig. 7 – Results of high pressure permeation test at 30 °C: influence of applied pressure on each value (a) Permeated hydrogen gas amount, (b) Permeability, (c) Diffusion, (d) Solubility. Measurement condition: transmission side area of high-low is 211 mm², nominal filtration accuracy is 1.0 μm.

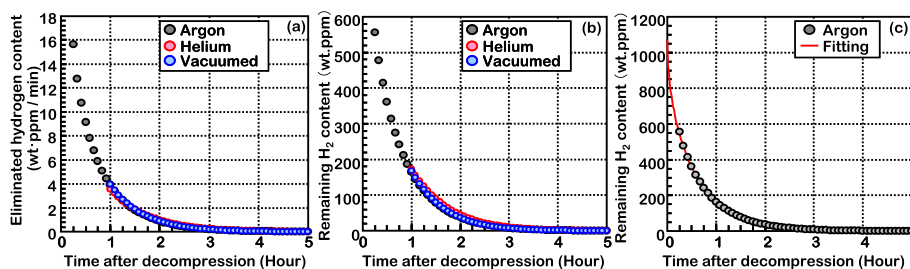


Fig. 8 – Influence of environments condition on remaining hydrogen content in specimens measured by argon carrier TDA after decompression following the hydrogen exposure to 90 MPa at 30 °C for 24 h “Argon” specimen is kept under argon environment 15 min after decompression, “Helium” and “Vacuumed” are kept under helium environments condition or vacuum condition 15 min after decompression and under argon environment 60 min after decompression. (a) Hydrogen elimination from the specimen (b) Profile of remaining hydrogen amount (c) Profile of remaining hydrogen amount under argon gas, and fitting with diffusion equation.

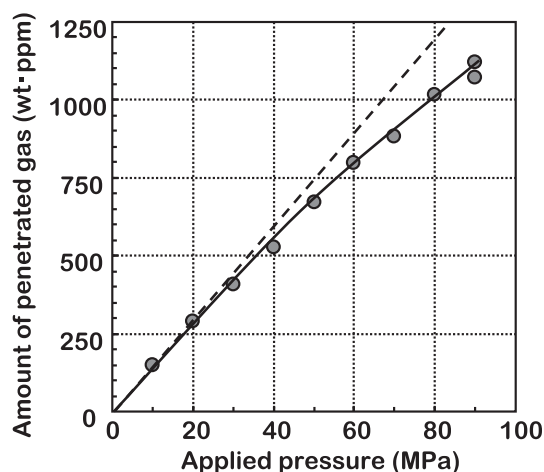


Fig. 9 – Pressure dependency of amount of penetrated hydrogen gas in HDPE determined by high-pressure permeation test.

elimination can be discussed with diffusion-controlling. The remaining hydrogen content extrapolated to zero hour is equivalent for the amount of penetrated gas under high-pressure equilibrium condition.

Fig. 9 shows the amount of penetrated gas in HDPE, which is the weight of the penetrated hydrogen per unit of HDPE weight, calculated based on the solubility coefficient obtained by the high-pressure permeation test method. As the test pressure increased, the absorption amount increased, but the ratio of increase slowed slightly as the pressure increased, and it was found that the pressure deviated from Henry's law.

Figs. 9(b) and 10(a) show correlations between amount of penetrated hydrogen gas and diffusion coefficients obtained by the TDA method. The amount of penetrated hydrogen gas showed the same tendency as those obtained with TDA measured at near non-equilibrium, but the diffusivity as a whole showed larger values with TDA. The amount of penetrated hydrogen measured by TDA and high-pressure hydrogen permeation test is considered to be the amount of hydrogen penetrates into a sample with shrinkage of free volume under pressure. As the specimens for both measurements are in the same hydrogen saturated state, the amount of

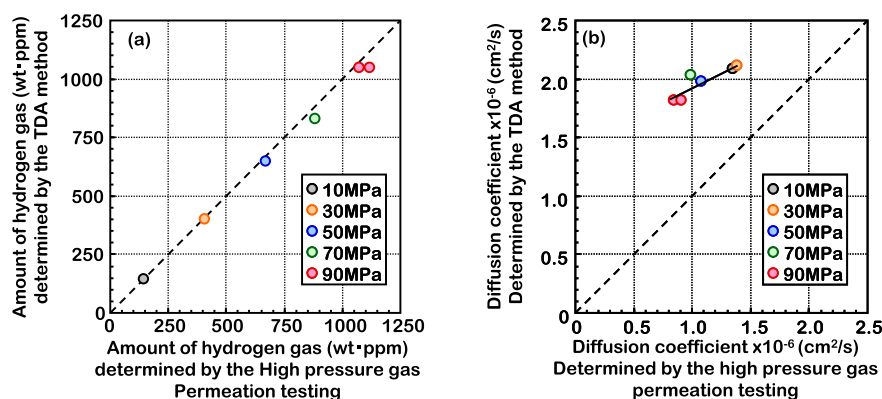


Fig. 10 – High-pressure hydrogen gas properties in HDPE using different measurements of equilibrium and no equilibrium States (a) Amount of penetrated hydrogen gas (b) Diffusion coefficient.

penetrated hydrogen shows the same value. In the high-pressure permeation test, the diffusion coefficient is measured in the steady state with shrunk free volume as it is, then the result reflects the behavior of the state with the decrease of the free volume. In contrast, the TDA method is a measurement in which the free volume recovers the state under atmospheric pressure, with the removal of external pressure. Because the diffusion coefficient is small when the free volume is small and large when the free volume is large, the TDA method shows a larger value than the high-pressure permeation test method. The higher the test condition pressure is, the greater the difference between the two results becomes. Therefore, it is inferred that the difference between the TDA method and the high-pressure permeation test method became smaller under the low-pressure condition, that is, the condition in which the diffusion coefficient is smaller.

Conclusion

An equipment capable of evaluating hydrogen permeation behavior of polymeric materials in an equilibrium state under high-pressure hydrogen gas conditions has been developed. The reliability of the equipment was ensured in terms of the accuracy in the measurement of the permeation area, permeation distance, avoiding the effect of filters, and keeping stability of pressure without gas leakage. The gas permeation amount in the environment up to 90 MPa was successfully measured, and the permeation coefficient was obtained. The diffusion coefficient, solubility coefficient, and gas penetration amount were calculated from the delay time. Precise and reliable values of those parameters are necessary to evaluate reliability of polymeric materials such as packing for hydrogen shut-off valves, O-Rings for joint sealing, backup rings, lining for hoses and tanks, multi layered materials, and the materials in which blister destruction progresses to conduct comparative analysis. The comparative analysis of the data earned by this method with the previously reported TDA data clarified that the diffusion coefficient was smaller than the TDA data, though the amount of penetrated hydrogen was almost same as in TDA data. Although TDA method has an advantage of simplicity and easiness for the measurement of amount of penetrated hydrogen gas, diffusion

behavior can not be analyzed, as it can be affected by the compression of the free volume due to hydrostatic pressure. The high-pressure permeation testing method we report in this paper enables to provide very accurate and precise data of permeation and diffusion coefficient and amount of penetrated hydrogen gas in high-pressure environment, which have been difficult to obtain. Those data are useful not only for selecting materials in the practical use under high-pressure hydrogen environment, but also for general theoretical discussions about penetration and diffusion of penetrant in polymer materials under a high-pressure environment. We will measure the size of shrunk free volume by utilizing the molecular size of penetrant, or the interaction of polymer materials with penetrant to discuss the permeation mechanism by using hydrogen, nitrogen, helium etc in high-pressure conditions. This method is expected to play an important role both in industrially and scientifically.

Declaration of competing interest

The authors declare that they have no known competing financial interests or personal relationships that could have appeared to influence the work reported in this paper.

Acknowledgment

A part of this research is based on the results obtained from a project commissioned by the New Energy and Industrial Technology Development Organization (NEDO), Japan.

Appendix

Influence of reading 7error in pressure gauge and thermometer on the results is shown in Table A3. Discrepancy of results are all negligibly small, supposing in 90 MPa case. The influence of $\pm 0.4\%$ error in applied pressure on permeation coefficient is $4.91\text{--}4.96 \times 10^{16} [\text{mol} \cdot \text{m}/(\text{m}^2 \cdot \text{s} \cdot \text{Pa})]$. The influence of $\pm 0.4\%$ error in thermometer on permeation coefficient is $4.94\text{--}4.96 \times 10^{16} [\text{mol} \cdot \text{m}/(\text{m}^2 \cdot \text{s} \cdot \text{Pa})]$ and amount of penetrated hydrogen is 1118–1121 wt · ppm.

Table A1 – High-pressure permeation test value.

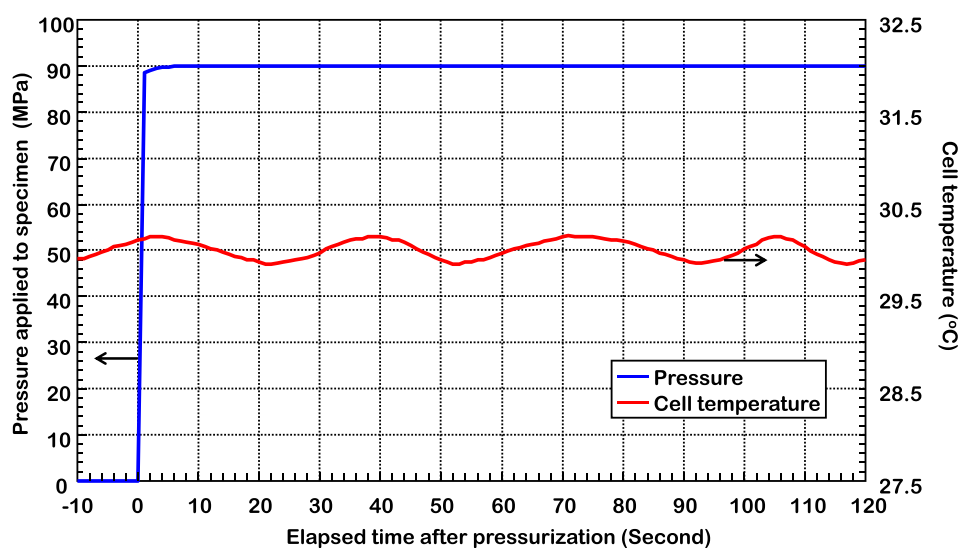
Target pressure [MPa]	Permeability coefficient [$\text{mol} \cdot \text{m}/(\text{m}^2 \cdot \text{s} \cdot \text{Pa})$ ($\times 10^{16}$)	Diffusion coefficient [cm^2/s] ($\times 10^6$)	Solubility coefficient [$\text{mol}/\text{m}^3 \cdot \text{Pa}$] ($\times 10^6$)	Amount of penetrated [wt · ppm]
10	9.25	1.35	6.87	143
20	8.78	1.32	6.65	289
30	8.05	1.28	6.28	409
40	7.40	1.20	6.17	526
50	6.76	1.08	6.25	671
60	6.32	1.01	6.25	799
70	5.88	0.99	5.96	881
80	5.40	0.90	6.00	1016
90	5.08	0.91	5.57	1073
90	4.95	0.84	5.86	1120

Table A2 – DATA measured by TDA mesod after high-pressure gas exposure

Target pressure [MPa]	Diffusion coefficient [cm ² /s] (x10 ⁶)	Amount of penetrated [wt· ppm]
10	2.09	143
30	2.11	401
50	1.98	646
70	2.03	831
90	1.82	1050

Table A3 – Influence of reading error in pressure gauge and thermometer

Factor of error	Pressure [MPa]	Temperature [°C]	Permeability coefficient [molm/(m ² · s · Pa)] (x10 ¹⁶)	Diffusion coefficient [cm ² /s] (x10 ⁶)	Solubility coefficient [mol/m ³ · Pa] (x10 ⁶)	Amount of penetrated [wt· ppm]
90 MPa/30 °C reference measurement results (actual measurement)	90.00	30.00	4.93	0.84	5.86	1120
When the pressure is different by + 0.45 MPa (assumption)	90.45	30.00	4.91	0.84	5.83	1120
When the pressure is different by –0.45 MPa (assumption)	89.45	30.00	4.96	0.84	5.90	1120
When the temperature is different by +0.5 °C (assumption)	90.00	30.50	4.93	0.84	5.85	1118
When the temperature is different by –0.5 °C (assumption)	90.00	29.50	4.94	0.84	5.87	1121

**Figure A1 – Conversion of pressure and temperature when right after measurement starts. Time zero corresponds to the time when Valve B opened.**

REFERENCES

- [1] Kiyoaki Onoue, Murakami Yukitaka, Petros Sofronis. Japan's energy supply: mid-to-long-term scenario -A proposal for a new energy supply system in the aftermath of the March 11 earthquake. *Int J Hydrogen Energy* 2012;37(10):8123–32.
- [2] IEA Technology roadmap - hydrogen and fuel cells. [http://ieahydrogen.org/pdfs/TechnologyRoadmapHydrogenandFuelCells-\(1\).aspx](http://ieahydrogen.org/pdfs/TechnologyRoadmapHydrogenandFuelCells-(1).aspx); 2015.
- [3] Mausae Steffen, Hapkeb Jobst, Ranongb Chakkrit Na, chnera Erwin Wü, Friedlmeiera Gerardo, Wenger David. Filling procedure for vehicles with compressed hydrogen tanks. *Int J Hydrogen Energy* 2008;33(17):4612–21.
- [4] Global technical regulation on hydrogen and fuel cell vehicles Contents. Global technical regulation No. 13. <https://www.unece.org/fileadmin/DAM/trans/main/wp29/wp29wgs/wp29gen/wp29registry/ECE-TRANS-180a13e.pdf>.
- [5] Adams P, Bengaouer A, Cariteau B, Molkov V, Venetsanos Allowable AG. Hydrogen permeation rate from road vehicles. *Int J Hydrogen Energy* 2011;36(3):2742–9.

- [6] Castagnet Sylvie, Grandidier Jean-Claude, Comyn Mathieu. Guillaume Benoit Hydrogen influence on the tensile properties of mono and multi-layer polymers for gas distribution. *Int J Hydrogen Energy* 2010;35(14):7633–40.
- [7] Prewitz Marc, Gaber Martin, Müller Ralf, Marotzke Christian, Holtappels Kai. Polymer coated glass capillaries and structures for high-pressure hydrogen storage: permeability and hydrogen tightness. *Int J Hydrogen Energy* 2018;43(11):5637–44.
- [8] B. Acosta, P. Moretto, N. Frischauf, F. Harskamp. Gastef: the JRC-IE compressed hydrogen gas tanks testing facility. <https://core.ac.uk/download/pdf/34994655.pdf>.
- [9] Koga Atsushi, Uchida Kenichi, Junichiro Yamabe, Shin Nishimura. Evaluation on high-pressure hydrogen decompression failure of rubber O-ring using design of experiments. *Int J Automot Eng* 2011;2(4):123–9.
- [10] Junichiro Yamabe, Koga Atsushi, Shin Nishimura. Failure behavior of rubber O-ring under cyclic exposure to high-pressure hydrogen gas. *Eng Fail Anal* 2013;35:193–205.
- [11] Junichiro Yamabe, Shin Nishimura. Influence of fillers on hydrogen penetration properties and blister fracture of rubber composites for O-ring exposed to high-pressure hydrogen gas. *Int J Hydrogen Energy* 2009;34(4):1977–89.
- [12] Koga Atsushi, Tadahisa Yamabe, Sato Hiroyuki, Uchida Kenichi, Nakayama Junichi, Junichiro Yamabe, Shin Nishimura. A visualizing study of blister initiation behavior by gas decompression. *Tribol Online* 2013;8(1):68–75.
- [13] Fujiwara Hirotada. Analysis of acrylonitrile butadiene rubber (NBR) expanded with penetrated hydrogen due to high pressure hydrogen exposure. *Int Polym Sci Technol* 2017;44(3):T41–8.
- [14] Fujiwara Hirotada, Ono Hiroaki, Shin Nishimura. Degradation behavior of acrylonitrile butadiene rubber after cyclic high-pressure hydrogen exposure. *Int J Hydrogen Energy* 2015;40(4):2025–34.
- [15] Ono Hiroaki, Fujiwara Hirotada, Kiyooki Onoue, Ono Hiroaki, Shin Nishimura. Influence of repetitions of the high-pressure hydrogen gas exposure on the internal damage quantity of high-density polyethylene evaluated by transmitted light digital image. *Int J Hydrogen Energy* 2019;44(41):23303–19.
- [16] Salame Morris. Prediction of gas barrier properties of high polymers. *Polym Eng Sci* 1986;26(22):1543–6.
- [17] Bicerano Jozef. Prediction of polymer properties. New York: Marcel Dekker; 1993. ISBN 0-203-91011-7.
- [18] Park JY, Paul DR. Correlation and prediction of gas permeability in glassy polymer membrane materials via a modified free volume based group contribution method. *J Membr Sci* 1997;125:23–39.
- [19] Li NN, Henley EJ. Permeation of gases through polyethylene films at elevated pressures. *AIChE J* 1964;10(5):666–70.
- [20] Reilly JW, Henley EJ, Staffin HK. Separation of gaseous mixtures by permeation through polyethylene film. *AIChE J* 1964;16(3):353–5.
- [21] Li NN, Long RB. Permeation through plastic films. *AIChE J* 1969;15(1):73–80.
- [22] Stern SA, Mullhaupt JT, Gareis PJ. The effect: of pressure on the permeation of gases and vapors through polyethylene. Usefulness of the corresponding states principle. *AIChE J* 1969;15(1):64–73.
- [23] Stern SA, Fang S-M, Frisch HL. Effect of pressure on gas permeability coefficients. A new application of "free volume" Theory. *J Poly Sci Part A-2* 1972;(10):201–19.
- [24] CO₂, CH₄, C₂H₄, and C₃H₈ Stern A, Kulkarni SS, Frisch HL. Tests of a "free-volume" model of gas permeation through polymer membranes. I. Pure CO₂, CH₄, C₂H₄, and C₃H₈ in polyethylene. *J Polym Sci Polym Phys Ed* 1983;21(3):467–81.
- [25] SF₆, CF₄, and C₂H₂F₂ Stern SA, Sampat SR, Kulkarni SS. Tests of a "free-volume" model of gas permeation through polymer membranes. II. Pure Ar, SF₆, CF₄, and C₂H₂F₂ in polyethylene. *J. Poly. Sci PART B Polym. Phys* 1986;24(10):2149–66.
- [26] Naito Yasutoshi, Mizoguchi Keishin, Terada Katsuhiko, Kamiya Yoshinori. The effect of pressure on gas permeation through semicrystalline polymers above the glass transition temperature. *J Polym Sci B Polym Phys* 1991;29(4):457–62.
- [27] Kamiya Yoshinori, Naito Yasutoshi, Bourbon Dominique. Sorption and partial molar volumes of gases in poly(ethylene-co-vinyl acetate). *J Polym Sci Polym Phys Ed* 1994;32(2):281–6.
- [28] Sato Yoshiyuki, Yurugi Masashi, Fujiwara Koji, Takishima Shigeki, Masuoka Hirokatsu. Solubilities of carbon dioxide and nitrogen in polystyrene under high temperature and pressure. *Fluid Phase Equil* 1996;125(1–2):129–38.
- [29] Sato Yoshiyuki, Iketani Toru, Takishima Shigeki, Masuoka Hirokatsu. Solubility of hydrofluorocarbon (HFC-134a, HFC-152a) and hydrochlorofluorocarbon (HCFC-142b) blowing agents in polystyrene. *Fluid Phase Equil* 1996;40(6):1369–75.
- [30] Sato Yoshiyuki, Takikawa Tadao, Sorakubo Atsushi, Takishima Shigeki, Masuoka Hirokatsu, Imaizumi Mitsuhiro. Solubility and diffusion coefficient of carbon dioxide in biodegradable polymers. *Ind Eng Chem Res* 2000;39(12):4813–9.
- [31] David C. Bonner Yang-leh Cheng A new method for determination of equilibrium sorption of gases by polymers at elevated temperatures and pressures. *J Polym Sci Polym Lett Ed* 1975;13(5):259–64.
- [32] Junichiro Yamabe, Nakao Masatoshi, Fujiwara Hirotada, Shin Nishimura. Influence of fillers on hydrogen penetration properties and blister fracture of EPDM composites exposed to 10 MPa hydrogen gas. *Nihon Kikai Gakkai Ronbunshu A Hen Trans Jpn Soc Mech Eng Part A* 2008;74(7):971e81.
- [33] Ono Hiroaki, Fujiwara Hirotada, Shin Nishimura. Penetrated hydrogen content and volume inflation in unfilled NBR exposed to high-pressure hydrogen. What are the characteristics of unfilled-NBR dominating them? *Int J Hydrogen Energy* 2019;44(41):23303–19.
- [34] Barrer RM. Permeation, diffusion and solution of gases in organic polymers. *Trans Faraday Soc* 1939;35:628–43.
- [35] Brubaker David William, Kammermeyer Karl. Flow of Gases through Plastic Membranes. *Indus Eng Chem* 1953;45(5):1148–52.
- [36] Van Amerongen GJ. The permeability of different rubbers to gases and its relation to diffusivity and solubility. *J Appl Phys* 1946;17(11):972–85.
- [37] Nagao Akihide, Takagi Shusaku. Gas-phase hydrogen permeation test device and method of protecting gas-phase hydrogen permeation test device United States patent patent. 2019; No.: US 10,295,453 B2.
- [38] SMC sintered metal element catalog. http://ca01.smcworld.com/catalog/en/ifilter_metal/EB-ES-E/6-11-p0103-0118-shouket_en/data/6-11-p0103-0118-shouket_en.pdf.
- [39] Stern SA, Fang S-M, Jobbins RM. Permeation of gases at high pressures. *J. Macromol. Sci Phys. B5* 1971;1:41–69.
- [40] Matsuzaki Yoshio, Kazamaki Tsuneji. Effect of surface roughness on compressive stress of static seals nippon kikai gakkai ronbunshu. *Chimia* 1987;53(489):1091–5.
- [41] Naito Yasutoshi, Bourbon Dominique, Terada Katsuhiko, Kamiya Yoshinori. Permeation of high-pressure gases in poly(ethylene-co-vinyl acetate). *J. Poly. Sci PART B Polym. Phys.* 1993;31:693–7.
- [41] Ito Taisuke, Marur Harumasa. Pressure-strain and pressure-volume relationships in the crystal lattice of polyethylene at 293 °K. *Polym J* 1971;2(6):768–82.